Available online at www.sciencedirect.com
SCIENCE DIRECT®
ELSEVIER
Journal of Environmental Radioactivity 73 (2004) 151–168
JOURNAL OF ENVIRONMENTAL RADIOACTIVITY
www.elsevier.com/locate/jenvrad

Environmental characterization and radio-ecological impacts of non-nuclear industries on the Red Sea coast

M.H. El Mamoney [a], Ashraf E.M. Khater [b,*]

[a] *National Institute of Oceanography & Fisheries, Alexandria, Egypt*
[b] *National Centre for Nuclear Safety and Radiation Control, Atomic Energy Authority, PO Box 7551, Nasr City, Cairo 11762, Egypt*

Received 1 January 2003; received in revised form 1 July 2003; accepted 23 August 2003

Abstract

The Red Sea is a deep semi-enclosed and narrow basin connected to the Indian Ocean by a narrow sill in the south and to the Suez Canal in the north. Oil industries in the Gulf of Suez, phosphate ore mining activities in Safaga—Quseir region and intensified navigation activities are non-nuclear pollution sources that could have serious radiological impacts on the marine environment and the coastal ecosystems of the Red Sea. It is essential to establish the radiological base-line data, which does not exist yet, and to investigate the present radio-ecological impact of the non-nuclear industries to preserve and protect the coastal environment of the Red Sea. Some natural and man-made radionuclides have been measured in shore sediment samples collected from the Egyptian coast of the Red Sea. The specific activities of ^{226}Ra and ^{210}Pb (^{238}U) series, ^{232}Th series, ^{40}K and ^{137}Cs (Bq/kg dry weight) were measured using gamma ray spectrometers based on hyper-pure germanium detectors. The specific activities of ^{210}Po (^{210}Pb) and uranium isotopes (^{238}U, ^{235}U and ^{234}U) (Bq/kg dry weight) were measured using alpha spectrometers based on surface barrier (PIPS) detectors after radiochemical separation. The absorbed radiation dose rates in air (nGy/h) due to natural radionuclides in shore sediment and radium equivalent activity index (Bq/kg) were calculated. The specific activity ratios of ^{228}Ra/^{226}Ra, ^{210}Pb/^{226}Ra, ^{226}Ra/^{238}U and ^{234}U/^{238}U were calculated for evaluation of the geo-chemical behaviour of these radionuclides. The average specific activity of ^{226}Ra (^{238}U) series, ^{232}Th series, ^{40}K and ^{210}Pb were 24.7, 31.4, 427.5 and 25.6 Bq/kg, respectively. The concentration of ^{137}Cs in the sediment samples was less than the lower limit of detection. The Red Sea coast is an arid

* Corresponding author. Present address: King Saud University, College of Science, Physics Dept., P.O. Box 2455, Riyadh 11451, Kingdom of Saudi Arabia. Tel.: +996 52 41 8292; fax: +996 14 67 3656.
E-mail address: khater_ashraf@yahoo.com (A.E.M. Khater).

0265-931X/$ - see front matter
doi:10.1016/j.jenvrad.2003.08.008

region with very low rainfall and the sediment is mainly composed of sand. The specific activity of ^{238}U, ^{235}U and ^{234}U were 25.3, 2.9 and 25.0 Bq/kg. The average specific activity ratios of $^{226}Ra/^{228}Ra$, $^{210}Pb/^{226}Ra$ and $^{234}U/^{238}U$ were 1.67, 1.22 and 1.0, respectively.

The relationship between $^{226}Ra/^{228}Ra$ activity ratio and sample locations along the coastal shoreline indicates the increase of this ratio in the direction of the Shuqeir in the north and Safaga in the south where the oil exploration and phosphate mining activities are located. These activities may contribute a high flux of ^{226}Ra. The concentration and distribution pattern of ^{226}Ra in sediment can be used to trace the radiological impact of the non-nuclear industries on the Red Sea coast.

Keywords: Natural radioactivity; Red Sea; Coastal environment; Non-nuclear industries

1. Introduction

Radionuclides have been an essential constituent of the earth since its creation. The earth's is still being heated through the decay of long-lived natural radionuclides e.g. uranium, thorium and potassium. All uses of natural or man-made radionuclides require an understanding of their environmental behaviour. Such knowledge is needed for their effective application as in-situ tracers or geo-chronometers and for estimation of human health risks. The advent of nuclear science resulted in the proliferation of nuclear applications and in the increase of environmental radioactivity levels. Further, we are exposed to radionuclides brought to the surface by man's traditional working activities such as mining operations and oil explorations, which have contributed to the increase of population radiation dose due to environmental radioactivity.

Egypt has about 700 km of coastline along the Red Sea proper, which is of great environmental, economical and recreational value. Commercial and subsistence fisheries provide a living for a large sector of the coastal population in Egypt. The eco-tourism infrastructure is continuously developing along the Egyptian Red Sea coast.

The Red Sea—Suez Canal pathway is one of the most important international marine pathways with highly intensive ship traffic. Some of these ships are running by nuclear power or carrying radioactive materials, which is a source of possible accidental contamination (Hawkins and Roberts, 1993).

In the Gulf of Suez, the northern part of the Red Sea, there are about 90% of the Egyptian oil exploration and production activities, which could be a significant source of environmental contamination with technological enhanced naturally occurring radioactive materials (TENORM).

On the Red Sea coast, there are two main centers for phosphate ore mining: Safaga and Quseir and three shipping harbours. Mining of the Red Sea coastal phosphorites began in 1910, for export to the Far East. The phosphatic deposits in the Quseir–Safaga district of the Red Sea coast are mined at many localities in the Quseir group of mines (Hamadat, Atshan, Duwi, Anz, Abu Tundub, Hamrawein), and at Safaga group of mines (Um El-Howeitat, Gasus, Wasif, Mohamed Rabah).

Phosphate ore dust spilled over into the Sea during shipping is considered as a continuous source for contaminating the Red Sea coastal environment (IOC, 1997 and Said, 1990).

There is a lack of information about the radioactivity levels and characterisation of the Egyptian Red Sea coastal environment. This information is essential to create a scientific database of the radiological base-line levels and to identify the radiological impacts of non-nuclear industries (e.g. phosphate mining, phosphate shipping and oil production activities) or any accidental contamination on the coastal region of the Red Sea.

The study on the concentrations of heavy metal pollution in the Egyptian Red Sea, over 50 years period (1934–1984), has shown that the concentrations of most of the heavy metals has increased, due to natural pollution from hot brine pools or due to man-made pollution from oil, heavy metal mining, discharge of domestic industrial wastes and phosphate mining and transportation along the Red Sea coastal areas (Hanna, 1992).

Our study is the first to focus on the spatial distribution pattern and levels of radioactivity in the Egyptian Red Sea coastal environment. These results will be useful to evaluate the present radio-ecological impacts of the non-nuclear industries (e.g. oil production and phosphate mining) on the coastal environment. Also, these data will be available for subsequent evaluations of the possible future environmental contamination due to the non-nuclear industries.

2. Material and methods

2.1. The study area

The Red Sea occupies an elongated escarpment-bounded depression, which extends in a south-east direction from Suez to the strait of Bab El-Mandeb in a nearly straight line. It separates the coasts of Arabia from those of Egypt, the Sudan and Ethiopia. Its total length is about 2200 km, and its breadth varies from 400 km in the southern half to 210 km in the north where it bifurcates into two arms, the Gulf of Suez and the Gulf of Aqaba (Said, 1990). The Red Sea is connected with the Mediterranean Sea by the Suez Canal, which has no locks; however, this connection is of no practical importance for exchange of water. In the south, the strait of Bab El-Mandeb limits water exchange between the Red Sea and the Gulf of Aden. The rainfall over the Red Sea and its coasts is extremely low. Evaporation exceeds precipitation, and this combined with the very restricted exchange of water with the open sea lead to the production of the dense, highly saline water (Khatir et al., 1998a,b).

The narrow coastal plain of the Egyptian Red Sea lies between the high fringing mountains consisting mostly of crystalline rocks and the seawater. Along the shores, there is an almost continuous band of emergent reef terraces between 0.5 and 10 km wide. Between these and the foot of the crystalline hills extends a sand gravel surface. The width of this plain ranges from less than 1 to 20 km. The main sources of sediments to the beaches of the Egyptian Red Sea are terrestrial deposits

transported from the fringing mountains during the occasional runoffs through the numerous wadis, and the Middle Miocene and later biogenic carbonate sediments (El Mamony and Rifaat, 2001).

2.2. Sampling and samples preparation

The samples were collected from the beach face along the entire area of study, which extended from Shuqeir north (latitude 28°3′39″ N) to Marsa Alam city south (Latitude 25°4′ 29″ N). Forty shore sediment samples were collected in 1997. The beach sediments in the study area are predominantly sand. The content of terrestrial deposit is the major control in determining the mean grain size of the sediment where most of the coarse sands are mainly quartz, feldspar and other silicate mineral grains. The samples were collected using a template of 25×25 cm^2 area and 5 cm depth (USDOE, 1992). The gravels size greater than 2 cm were discarded. The sampling locations are shown in Fig. 1. The geographical description of sampling locations: samples density (kg/l), mean grain size, and sorting; CO_3%, Ba (ppm) and Sr (ppm) in the collected samples are given in Table 1 (El Mamony and Rifaat, 2001). The collected samples were dried at 110 °C, pulverised, homogenised and sieved through a 2 mm mesh. For uranium isotopes analysis portions

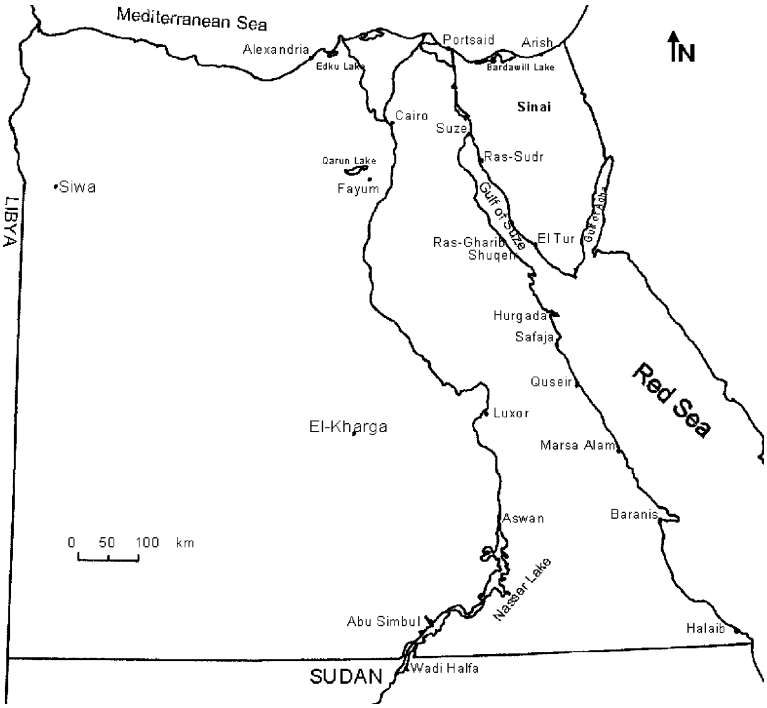

Fig. 1. Map of Egypt and the studied area of the Red Sea Egyptian coast.

Table 1
Geographic description of sampling locations; samples density (g/ml), mean grain size (phi), and sorting; CO_3 (%), Ba (ppm) and Sr (ppm) in shore sediment samples of the Red Sea coast (El Mamony and Rifaat, 2001)

Ser.	CODE	Location	N (Deg. Min. s)	E (Deg. Min. s)	Density (g/ml)	Mean grain size	Sorting	CO_3 (%)	Ba (ppm)	Sr (ppm)
1	453	Shuqeir	28 03 39	33 20 09	1.42	Very coarse sand	Moderately well sorted	40.8	2093	4037
2	455	South Shuqeir	28 00 48	33 26 23	1.56	Medium sand	Moderately well sorted	57.7	2757	6755
3	456	South Shuqeir	27 58 09	33 29 52	1.70	Very coarse sand	Very well sorted	16.9	778	1232
4	458	South Ras El'Esh	27 52 07	33 33 44	1.50	Very coarse sand	–	13.2	227	1078
5	459	Gebel El'Zeit	27 49 51	33 34 51	1.80	Coarse sand	Moderately sorted	38.5	1551	3987
6	461	Gebel El'Zeit	27 47 55	33 29 22	1.52	Very coarse sand	Moderately well sorted	28.0	2084	1561
7	462	Gebel El'Zeit	27 45 00	33 31 38	1.69	Medium sand	Moderately well sorted	8.7	3170	483
8	463	Ras El'Esh	27 44 01	33 32 54	1.53	Medium sand	Moderately sorted	55.0	1538	7176
9	464	Ras Jemsha	27 41 01	33 33 22	1.60	Medium sand	Very well sorted	3.5	184	108
10	468	50 km North Hurghada	27 37 05	33 32 11	1.68	Medium sand	Poorly sorted	34.1	1690	4495
11	469	40 km North Hurghada	27 34 05	33 33 57	1.63	Medium sand	Moderately sorted	23.0	1834	3741
12	470	35 km North Hurghada	27 31 34	33 33 44	1.60	Medium sand	Moderately well sorted	6.5	393	484
13	471	–	–	–	1.53	–	–	–	–	–
14	473	27 km North Hurghada	27 26 36	33 39 14	1.54	Medium sand	Moderately sorted	22.4	951	2668
15	474	–	27 15 34	33 48 43	1.48	–	–	–	–	–
16	475	20 km North Hurghada	27 21 38	33 41 07	1.64	Medium sand	Moderately sorted	20.2	1192	2729
17	476	15 km North Hurghada	27 17 34	33 45 43	1.84	Fine sand	Moderately well sorted	13.7	1706	1207
18	501	12 km North Hurghada	27 07 14	33 49 44	1.8	Medium sand	Moderately sorted	20.7	2273	1931
19	505	Sharm El'Arab	26 58 00	33 55 17	1.76	Medium sand	Moderately sorted	16.0	3021	2114
20	507	Sharm El'Naga	26 53 57	33 57 48	1.61	Medium sand	Moderately well sorted	9.5	3162	894
21	508	Ras Abu Suma	26 50 51	33 59 17	1.76	Medium sand	Moderately well sorted	21.5	2693	3229
22	509	Abu Suma Bay	26 50 11	33 56 58	1.68	Fine sand	Moderately sorted	19.6	2336	3983
23	510	7 km North Safaga	26 47 10	33 56 15	1.70	Coarse sand	Moderately sorted	2.9	ND	ND
24	511	Safaga City	26 43 18	33 56 14	1.70	Medium sand	Poorly sorted	27.6	2813	3128
25	512	5 km South Safaga	26 40 39	33 56 03	1.72	Medium sand	Moderately well sorted	22.6	1896	3701
26	515	20 km South Safaga	26 33 59	34 02 06	1.50	Medium sand	Moderately well sorted	43.8	2247	4647
27	518	40 km North Quseir	26 25 42	34 06 09	1.50	Medium sand	Poorly sorted	56.6	3394	6338
28	522	20 km North Quseir	26 15 10	34 12 07	1.60	Fine sand	Well sorted	25.7	3217	3996
29	524	10 km North Quseir	26 09 55	34 14 37	1.35	Medium sand	Poorly sorted	79.6	5450	8073

(continued on next page)

Table 1 (*continued*)

Ser.	CODE	Location	N (Deg. Min. s)	E (Deg. Min. s)	Density (g/ml)	Mean grain size	Sorting	CO_3 (%)	Ba (ppm)	Sr (ppm)
30	528	14 km South Quseir	26 00 21	34 20 03	1.62	Coarse sand	Moderately sorted	92.0	3766	6467
31	530	25 km South Quseir	255	34 23 42	1.66	Medium sand	Moderately well sorted	57.7	4923	8034
32	531	36 km South Quseir	25 53 16	34 24 43	1.74	Medium sand	Poorly sorted	59.3	3898	4787
33	534	45 km South Quseir	25 46 04	34 30 53	1.30	Medium sand	Moderately well sorted	70.9	4863	5920
34	536	55 km South Quseir	25 41 15	34 33 50	1.58	Fine sand	Moderately sorted	32.9	966	3353
35	538	Umm Qirayfat (67 km South Quseir)	25 36 31	34 36 17	1.56	Coarse sand	Well sorted	63.4	3162	5651
36	541	82 km South Quseir	25 28 45	34 40 36	1.80	Fine sand	Moderately well sorted	38.5	1479	5418
37	545	28 km North Marsa Alam	25 18 51	34 45 01	1.50	Fine sand	Moderately well sorted	11.5	1431	740
38	548	14 km North Marsa Alam	25 11 42	34 49 20	1.54	Fine sand	Moderately well sorted	42.8	5394	5209
39	549	9 km NorthMarsa Alam (Wadi Aslai)	25 09 26	34 51 06	1.62	Medium sand	Moderately well sorted	48.9	1826	5536
40	551	Marsa Alam City	25 04 29	34 53 52	1.72	Medium sand	Moderately well sorted	22.8	2087	1153

of the dried samples were moistured with concentrated nitric acid, fumed off to dryness, and ashed at 550 °C for about 12 h (Khater, 1997).

2.3. Analytical techniques

2.3.1. Gamma spectrometric analysis

The dried samples were transferred to polyethylene containers of 100 cm^3 capacity and sealed at least for 4 weeks to reach secular equilibrium between radium and thorium, and their progenies. ^{226}Ra (^{238}U) series, ^{232}Th series, ^{40}K, ^{137}Cs and ^{210}Pb specific activities were measured using well-calibrated gamma spectrometry based on hyper-pure germanium (HpGe) detectors. The HpGe detector had a relative efficiency of 40% and full width at half maximum (FWHM) of 1.95 keV for ^{60}Co gamma energy line at 1332 keV. The gamma transmissions used for activity calculations are 352.9 (^{214}Pb), 609.3, 1120.3 and 1764.5 keV (^{214}Bi) for ^{226}Ra (^{238}U) series, 338.4, 911.1 and 968.9 keV (^{228}Ac) for ^{232}Th series, 1460.7 keV for ^{40}K, 661.6 keV for ^{137}Cs and 46.5 keV for ^{210}Pb. The gamma spectrometers were calibrated using both ^{226}Ra point source and potassium chloride standard solutions in the same geometry as the samples (Khater, 1997). The lower limits of detection, with 95% confidence, for ^{226}Ra, ^{232}Th and ^{40}K are 0.28, 0.16 and 1.0 Bq/kg, respectively for 20 h counting time and 1 l sample volume (Currie, 1968).

2.3.2. Uranium isotopes analysis

Ashed samples (2–5 g) were spiked, for chemical recovery and activity calculations, with about 70 mBq ^{232}U tracer and dissolved using mineral acids (HNO_3, HF and HCl). Uranium was extracted with trioctylphosphine oxide in cyclohexane, back-extracted with NH_4F/HCl solution, then co-precipitated with $La(NO_3)_3$ and purified by passing through an anion exchange column. Uranium was electroplated on a stainless-steel disk from oxalate–chloride solution. The prepared samples were measured using alpha spectrometry (CANBERRA 4701 vacuum chambers) based on surface barrier (PIPS) detectors with 450 mm^2 surface area, about 25% efficiency and about 20 keV resolution, and connected up to a computerised multichannel analyser operating with Genie 2000 software (CANBERRA). The lower detection limit of the procedure is about 1 mBq/sample (1000 min measuring time) (Pimpl et al., 1992). The chemical recovery was in the range of 40–70%.

2.3.3. Lead-210–Polonium-210 analysis

Dried samples (1–2 g) were spiked, for chemical recovery and activity calculation, with about 80 mBq ^{208}Po and dissolved using mineral acids (HNO_3, HF and HCl). Finally, the samples residuals were dissolved in 30 ml of 0.5 M HCl. About 100 mg of ascorbic acid was added to the hot solution to reduce the iron content. Then, polonium was self-plated from the solution at temperatures between 80 and 90 °C onto rotating stainless steel disk fixed in a Teflon disk holder (Hamilton and Smith, 1986). The plated disks were measured using alpha spectrometers described above. The samples were measured for 1000 min, applying a lower limit of detection of 1 mBq (Currie, 1968). The average chemical recovery was 75%, and

the individual values ranged from 50 to 100%. The measured ^{210}Po specific activity is equivalent to ^{210}Pb specific activity.

2.4. Theoretical calculations

Radium equivalent activity (Bq/kg) is an index which is convenient to compare the specific activities of samples containing different concentrations of ^{226}Ra, ^{232}Th and ^{40}K. It is defined based on the assumption that 10 Bq ^{226}Ra/kg, 7 Bq ^{232}Th/kg and 130 Bq ^{40}K/kg produce the same gamma dose rate. It is calculated using the following equation:

$$\mathrm{Ra_{eq}} = C_{\mathrm{Ra}} + \frac{10}{7} C_{\mathrm{Th}} + \frac{10}{130} C_{\mathrm{K}}$$

Where C_{Ra}, C_{Th} and C_{K} are activity concentrations (Bq/kg dry weight) of ^{226}Ra, ^{232}Th and ^{40}K, respectively (Khater, 1997).

Absorbed dose in air (nGy/h) 1 m above the ground surface due to natural radionuclides (^{226}Ra series, ^{232}Th series and ^{40}K) in shore sediment was calculated using the following equation (UNSCEAR, 2000):

$$D\ (\mathrm{nGy/h}) = 0.462 C_{\mathrm{Ra}} + 0.604 C_{\mathrm{Th}} + 0.042 C_{\mathrm{K}}$$

Where C_{Ra}, C_{Th} and C_{K} are the specific activities (Bq/kg dry weight) of ^{226}Ra, ^{232}Th and ^{40}K, respectively.

3. Results and discussion

Activity concentrations of ^{226}Ra (^{238}U) series, ^{232}Th series, ^{40}K, and ^{210}Pb (Bq/kg dry weight) in the shore sediment samples are shown in Table 2. The average ac tivity ± standard error (range) of ^{226}Ra (^{238}U) series, ^{232}Th series, ^{40}K, ^{210}Pb (gamma) and ^{210}Pb(alpha) were 24.7 ± 4.3 (5.3–105.6), 31.4 ± 9.41 (2.34–221.9), 42 7.5 ± 35.5 (97.58–1011.3), 25.6 ± 3.9 (7.1–81.8) and 23.9 ± 3.7 (8.1–96.0) Bq/kg dry weight, respectively.

The range of measured activities differed widely as their presence in marine environment depends on their physical, chemical and geo-chemical properties and the pertinent environment (Khatir et al., 1998a,b). In coastal waters, it can be assumed that the mineral fraction of the sediment has uranium and thorium contents similar to those of terrestrial rocks (Strezov et al., 1996).

The average activities (range) of ^{226}Ra (^{238}U) series, ^{232}Th series and ^{40}K in Egyptian soil are 17 (5–64), 18 (2–96) and 320 (29–650) Bq/kg dry weight, respectively (UNSCEAR, 2000).

The activity of caesium-137 in the shore sediment samples was less than the lower limit of detection (0.1 Bq/kg, for 12 h measuring time) (Currie, 1968). This could be because the coastal region of the Red Sea is free from any direct anthropogenic radioactive waste discharge; it has an arid region with extremely low rainfall, and is composed mainly of sand, which has low adsorption capacity. The average activity of ^{137}Cs in bottom sediment of Sudanese Red Sea coast is 4.1 Bq/kg (Khatir et al., 1998a,b). It is less than the values from the pre-Chernobyl

Table 2
Specific activity (Bq/kg dry weight) of Ra-226 series, Th-232 series, K-40 and Pb-210 in shore sediment samples of Red Sea coast

Ser.	Code	Ra-226 ± E	Th-232 ± E	K-40 ± E	Pb-210[a] ± E	Pb-210[b] ± E[c]
1	453	8.95 ± 1.27	3.32 ± 1.55	425.17 ± 13.05	–	10.24 ± 0.64
2	455	6.05 ± 1.29	4.27 ± 0.70	97.58 ± 6.96	7.90 ± 0.79	8.07 ± 0.70
3	456	18.14 ± 0.89	13.95 ± 1.09	634.33 ± 6.09	13.95 ± 1.37	18.78 ± 1.18
4	458	31.59 ± 3.22	18.49 ± 2.91	1011.30 ± 27.73	22.05 ± 3.58	17.54 ± 1.34
5	459	11.91 ± 0.90	5.69 ± 1.11	377.02 ± 6.64	9.88 ± 1.02	15.71 ± 0.79
6	461	12.29 ± 1.14	10.95 ± 1.29	620.96 ± 11.23	19.50 ± 1.94	16.09 ± 1.32
7	462	9.67 ± 1.08	6.37 ± 1.75	616.30 ± 10.68	<LLD	10.98 ± 0.94
8	463	5.53 ± 0.32	5.59 ± 0.45	370.87 ± 5.30	9.44 ± 0.78	13.86 ± 1.09
9	464	8.51 ± 0.85	4.56 ± 0.76	401.00 ± 0.76	–	–
10	468	9.08 ± 0.90	7.62 ± 0.88	435.63 ± 7.93	–	11.95 ± 0.99
11	469	20.30 ± 1.44	15.63 ± 1.24	457.15 ± 9.23	11.08 ± 0.98	17.97 ± 1.31
12	470	9.60 ± 2.21	8.10 ± 2.64	376.16 ± 15.37	13.54 ± 1.42	14.49 ± 1.20
13	471	9.97 ± 1.47	6.57 ± 1.32	524.89 ± 13.91	7.08 ± 0.90	12.38 ± 1.27
14	473	11.16 ± 1.01	9.28 ± 1.02	394.84 ± 7.62	14.07 ± 1.22	14.83 ± 1.19
15	474	–	–	–	–	10.30 ± 0.91
16	475	50.25 ± 1.25	132.46 ± 1.81	587.70 ± 7.17	29.34 ± 3.40	73.35 ± 3.40
17	476	87.32 ± 2.19	221.90 ± 3.52	377.02 ± 8.93	77.30 ± 7.73	–
18	501	105.56 ± 2.99	205.17 ± 4.15	572.92 ± 13.81	48.85 ± 11.67	–
19	505	37.87 ± 1.53	66.31 ± 2.52	725.10 ± 12.04	50.51 ± 5.56	–
20	507	96.22 ± 2.25	143.61 ± 2.89	725.16 ± 27.40	80.99 ± 3.13	96.01 ± 5.71
21	508	14.19 ± 1.16	15.01 ± 1.16	635.75 ± 8.90	19.76 ± 2.17	25.42 ± 2.89
22	509	–	–	–	–	22.93 ± 1.43
23	510	22.08 ± 2.12	18.67 ± 2.47	886.50 ± 14.20	10.46 ± 1.10	–
24	511	67.75 ± 2.44	12.72 ± 2.79	485.30 ± 12.15	81.75 ± 5.09	81.41 ± 4.32
25	515	11.13 ± 1.05	2.34 ± 0.88	310.48 ± 8.01	23.71 ± 2.61	13.39 ± 1.49
26	518	14.67 ± 2.47	8.90 ± 2.92	282.08 ± 12.69	<LD	8.67 ± 0.92
27	522	18.70 ± 1.46	4.00 ± 0.87	253.66 ± 9.58	29.63 ± 2.04	32.68 ± 1.68
28	524	6.5 ± 1.1	<DL	128.14 ± 7.53	8.72 ± 1.05	12.29 ± 1.35
29	528	16.28 ± 0.99	4.53 ± 1.03	224.55 ± 6.36	25.61 ± 2.59	31.61 ± 4.71
30	530	33.07 ± 1.05	33.86 ± 1.47	136.27 ± 5.85	28.56 ± 2.23	–
31	531	44.38 ± 1.98	37.08 ± 2.15	313.54 ± 10.54	–	23.41 ± 1.54
32	534	8.26 ± 0.76	4.59 ± 2.27	194.48 ± 6.32	16.93 ± 1.76	22.04 ± 1.91
33	536	17.66 ± 1.39	9.69 ± 1.43	434.68 ± 10.56	14.82 ± 1.84	23.26 ± 1.12
34	538	5.32 ± 0.92	3.34 ± 1.31	294.70 ± 9.87	11.40 ± 1.39	23.31 ± 2.36
35	541	27.22 ± 4.28	32.69 ± 4.06	118.28 ± 7.10	29.63 ± 3.26	34.75 ± 2.61
36	545	9.99 ± 1.34	9.70 ± 1.90	257.26 ± 8.36	23.71 ± 3.01	17.00 ± 1.64
37	548	10.39 ± 1.66	5.48 ± 2.42	444.60 ± 17.23	11.85 ± 1.19	–
38	549	9.62 ± 1.0	6.92 ± 2.03	257.81 ± 6.99	14.63 ± 1.46	14.51 ± 0.87
39	551	–	–	–	–	14.61 ± 1.37

[a] Pb-210 Gamma analysis.
[b] Pb-210 alpha analysis.
[c] Error (statistical and counting error only).

period cited in the literature for marine sediments from different regions of the world (Khater, 1997; Khatir et al., 1998a,b; El Mamony and Rifaat, 2001).

Relationships between ^{226}Ra and ^{232}Th, ^{40}K, ^{210}Pb, and Ba concentrations in the Red Sea shore sediment samples are given in Fig. 2. The relationships between

^{226}Ra and ^{232}Th, and ^{210}Pb were strongly correlated with correlation coefficients (R) values of 0.89 and 0.91, respectively. These strong correlations could be because Ra and Th have some similarity in their environmental origin, i.e. the rocks from which the shore sediment were formed, and their chemical behaviour, while ^{210}Pb is a decay product of ^{222}Rn gas, which is a daughter of ^{226}Ra. The relationships between ^{226}Ra and ^{40}K and Ba were weak with correlation coefficient (R) values of 0.31 and 0.01, respectively. The weak correlation between radium and potassium could be explained due to the high potassium solubility. While the weak correlation between radium and barium could be due to the possible input of barium as a result of oil exploration activities in the Northern region, i.e. barium-bearing mud used during drilling operations of oil wells and possible input of radium as a result of phosphate mining activities (Khater et al., 2001; El Mamoney and Rifaat, 2001; Shawky et al., 2001). Vegueria et al. (2002) showed strong correlation between radium isotopes and barium in the water produced from offshore petroleum platforms.

The activity ratios of ^{226}Ra/^{228}Ra, ^{210}Pb (gamma)/^{226}Ra, ^{210}Pb(alpha)/^{226}Ra, ^{210}Pb(alpha)/^{210}Pb(gamma), and radium equivalent activity (Bq/kg) and absorbed

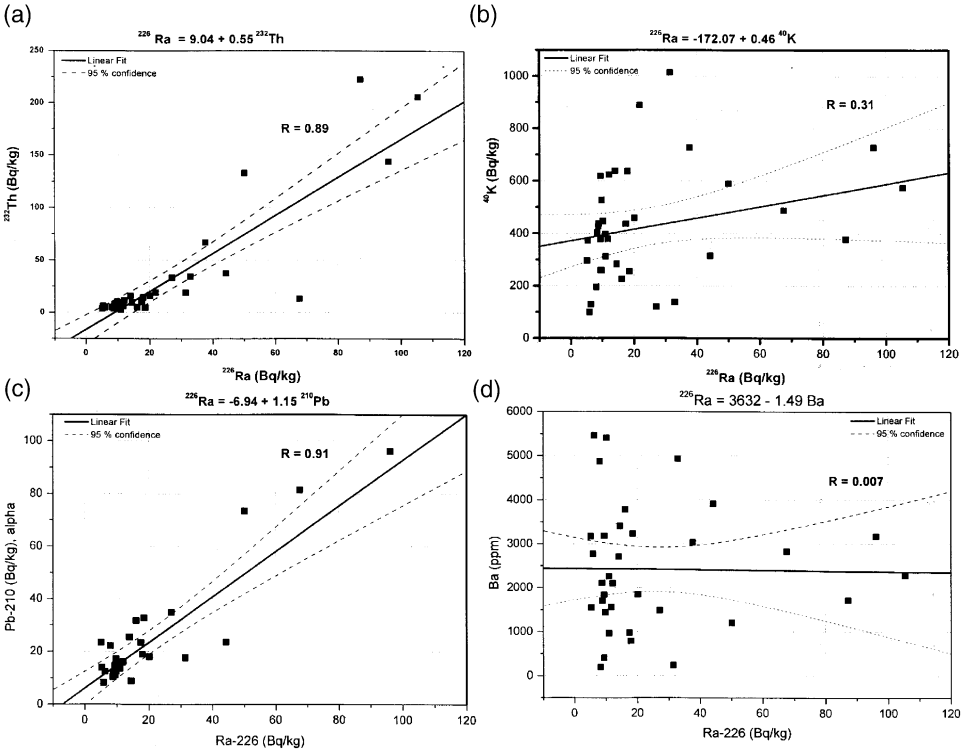

Fig. 2. Relationships Between ^{226}Ra and ^{232}Th (A), ^{40}K (B), ^{210}Pb (C) and Ba (D) concentrations in the Red Sea shore sediment samples.

dose rate in air (nGy/h) are given in Table 3. The average activity ratios ± standard error (range) of $^{226}Ra/^{228}Ra$, $^{210}Pb(gamma)/^{226}Ra$, $^{210}Pb(alpha)/^{226}Ra$ and $^{210}Pb(alpha)/^{210}Pb(gamma)$ were 1.67 ± 0.02 (0.38–5.33), 1.22 ± 0.10 (0.46–2.37), 1.48 ± 0.14 (0.53–4.38) and 1.28 ± 0.09 (0.56–2.5), respectively. The average radium equivalent activity (Bq/kg) and absorbed dose rate in air (nGy/h) ±

Table 3
Specific activity ratios of Ra-226/Ra-228, Pb-210/Ra-226 and Pb-210 (alpha analysis)/Pb-210 (gamma analysis), radium equivalent activity (Bq/kg) and absorbed dose rate (nGy/h) in shore sediment samples of the Red Sea coast

Ser.	Code	Ra-226/ Ra-228	Pb-210[a]/ Ra-226	Pb-210[b]/ Ra-226	Pb-210[b]/ Pb-210[a]	Radium— equivalent	nGy/h
1	453	2.70	–	1.14	–	46.40	23.21
2	455	1.42	1.31	1.33	1.02	19.65	8.60
3	456	1.30	0.77	1.04	1.35	86.86	40.50
4	458	1.71	0.70	0.56	0.80	135.80	64.27
5	459	2.09	0.83	1.32	1.59	49.04	23.53
6	461	1.12	1.59	1.31	0.83	75.70	36.02
7	462	1.52	–	1.14	–	66.18	32.75
8	463	0.99	1.71	2.51	1.47	42.04	20.29
9	464	1.87	–	–	–	45.87	22.50
10	468	1.19	–	1.32	–	53.48	25.45
11	469	1.30	0.55	0.89	1.62	77.79	34.79
12	470	1.19	1.41	1.51	1.07	50.11	23.41
13	471	1.52	0.71	1.24	1.75	59.72	29.16
14	473	1.20	1.26	1.33	1.05	54.78	25.39
15	475	0.38	0.58	1.46	2.50	284.69	101.5
16	476	0.39	0.89	–	–	433.32	146.15
17	501	0.51	0.46	–	–	442.73	155.96
18	505	0.57	1.33	–	–	188.38	74.65
19	507	0.67	0.84	1.00	1.19	357.17	133.00
20	508	0.95	1.39	1.79	1.29	84.54	39.16
21	510	1.18	0.47	–	–	116.94	54.75
22	511	5.33	1.21	1.20	1.00	123.24	56.70
23	515	4.76	2.13	1.20	0.56	38.36	19.04
24	518	1.65	–	0.59	–	49.09	22.15
25	522	4.67	1.58	1.75	1.10	43.92	20.84
26	524	–	1.34	1.89	1.41	16.36	8.35
27	528	3.59	1.57	1.94	1.23	40.02	18.72
28	530	0.98	0.86	–	–	91.92	34.71
29	531	1.20	–	0.53	–	121.47	48.63
30	534	1.80	2.05	2.67	1.30	29.78	13.79
31	536	1.82	0.84	1.32	1.57	64.94	30.22
32	538	1.60	2.14	4.38	2.04	32.75	16.10
33	541	0.83	1.09	1.28	1.17	83.02	30.78
34	545	1.03	2.37	1.70	0.72	43.63	19.28
35	548	1.90	1.14	–	–	52.41	25.56
36	549	1.39	1.52	1.51	0.99	39.35	18.01

[a] Pb-210 gamma analysis.
[b] Pb-210 alpha analysis.

standard error (range) were 101.2 ± 18.0 (16.4–442.7) and 41.6 ± 6.15 (8.35–155.96), respectively.

The relationships between $^{226}Ra/^{228}Ra$ and samples locations are given in Fig. 3. These relationships and their trend lines imply the increase of $^{226}Ra/^{228}Ra$ activity ratio in the direction of Shuqeir in the North and Safaga where the oil exploration and phosphate mining activities are located.

The lowest activity ratios of $^{226}Ra/^{228}Ra$ and the highest radium equivalent activity and absorbed dose rate were found in the Hurghada—Sharm El-Naga region (sample codes, 475–507) with average values of 0.51, 341.3 Bq/kg and 122.3 nGy/h, respectively. These high values could be explained due to the presence of black sands, which are enriched in the mineral monazite containing a significant amount of ^{232}Th (^{228}Ra). The enrichment occurs because the specific gravity of monazite allows its concentration along beaches where lighter materials are swept away (Cowart and Burnett, 1994).

The average value of $^{232}Th/^{238}U$ ($^{228}Ra/^{226}Ra$, assuming the secular equilibrium between ^{238}U series and ^{232}Th series and their progenies) activity ratios are 12.35 in pure monazite samples prepared from beach sand of Rosette and 1.4 in beach sand

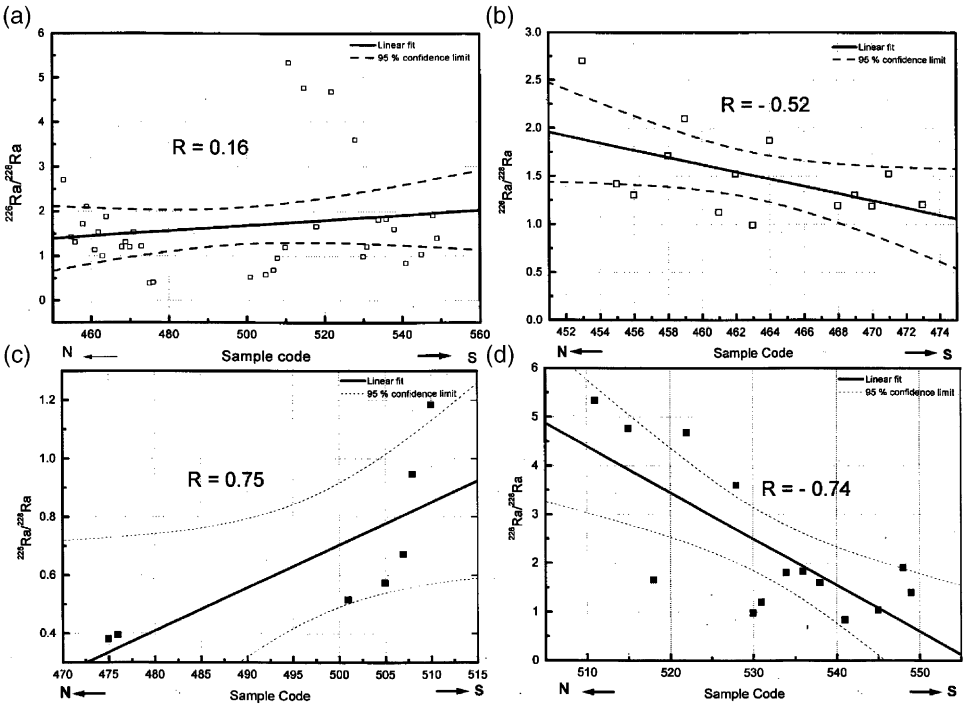

Fig. 3. Relationships between $^{226}Ra/^{228}Ra$ activity ratio and sample location (Code): (a) Shuqeir–Marsa Alam, (b) Shuqeir–Hurghada, (c) Hurghada–Safaga, and (d) Safaga–Marsa Alam.

of Rosetta-Egypt. This sand consists of monazite, zircon, thorite, garnet, rutile and other heavy mineral grains. The monazite sand contains high concentration of uranium and thorium, which gave the highest calculated dose rate found there (Ibrahiem et al., 1993; UNSCEAR, 2000).

The average activity ratio (range) of $^{226}Ra/^{228}Ra$ in the north part of the Red Sea (sample codes from 453 to 473) is 1.5 (0.99–2.7). The increase of these ratios above the unity could be attributed to the oil exploration and production processes, and/or to their geo-chemical behaviour in the environment.

The average activity ratio (range) of $^{226}Ra/^{228}Ra$ in the region of Safaga–Quseir–Marsa Alam city (sample codes from 510 to 549) was 2.25 (0.83–5.33). The increases of these ratios, exceeding unity, could be attributed to the phosphate mining in Safaga–Quseir region and/or their geo-chemical behaviour in the environment.

Radium is chemically similar to barium and with lesser degree to calcium (Cowart and Burnett, 1994). The previous study on barium concentrations in Red Sea shore sediment samples showed that non-carbonate barium (Ba/CO_3) increases from south (Marsa Alam) to north (Shuqeir) at which oil exploration and production processes are present. Oil exploration in the Egyptian Red Sea is mainly restricted to the Gulf of Suez and the northern part of the Red Sea proper. The effect of barium-bearing mud used during drilling operations of oil wells is prominent at Shuqeir City. Other sources of barium could be neglected (El Mamoney and Rifaat, 2001).

In Safaga–Qusier region (sample codes 512–528), the average activity ratio of $^{226}Ra/^{228}Ra$ was 3.68. The average radium equivalent activity and dose rate were 37.55 Bq/kg and 13.88 nGy/h, respectively; much lower than the average values and that of the Hurghada–Sharm El-Naga region. The high average activity ratio of $^{226}Ra/^{228}Ra$ could be explained due to the phosphate mining activities in Safaga–Quseir region where the concentration of ^{238}U and its decay products tend to be elevated in phosphate deposits (Khater et al., 2001; NAS, 1999). The average absorbed dose rate in air due to natural radionuclides in the Egyptian soil is 51 and 20–400 nGy/h in areas of high natural radiation background (Monazite sands) (UNSCEAR, 2000).

The average activity ratio of ^{210}Pb (alpha)$/^{226}Ra$ is greater than unity, 1.48, and ranged from 0.53 to 4.38. Radium-226 is decaying to ^{222}Rn gas, which is emanating from the geological formation depending on the porosity of the matrix. The mobility of the radon is regarded as one of the main causes of disequilibrium in the uranium decay series (Ivanovich and Harmon, 1992). Also, the ^{210}Pb (^{222}Rn decay product) fallout flux from the atmosphere and/or geo-chemical behaviour of both Pb and Ra in the environment could explain uranium series (U–Ra–Pb) disequilibrium in the environment. Radium forms a complex with chloride and in this form is quite mobile. Conversely, even moderate amounts of sulfate ion inhibit transport because of the co-precipitation of radium sulfate along with barium sulfate. Almost all lead salts are insoluble or sparingly soluble in water (Cowart and Burnett, 1994).

The specific activity of ^{210}Pb was measured using two measuring techniques (directly by gamma spectrometry and through ^{210}Po measurement by alpha spectrometry after radiochemical preparation). The results of both techniques are correlated (correlation coefficient = 0.9). The average activity ratio of $^{210}Pb_{alpha}/^{210}Pb_{gamma} \pm$ standard error (range) was 1.28 ± 0.09 (0.56–2.5). This deviation from unity could be due to low emission rate and a high self-absorption within the sample matrix of the ^{210}Pb soft gamma ray transition at 46.5 keV. Such self-absorption correction is difficult due to its high degree of dependence on the mineralogical composition of the sample (Hussain et al., 1996).

The activities (Bq/kg dry weight) of ^{238}U, ^{235}U, ^{234}U and total uranium, and activity ratios of $^{234}U/^{238}U$, $^{226}R/^{238}U$ and $^{210}Pb/^{238}U$ are shown in Table 4. The activity (Bq/kg dry weight) $\pm$ standard error (range) of ^{238}U, ^{235}U, ^{234}U and total U were 25.25 ± 6.82 (9.72–61.98), 2.94 ± 0.33 (2.41–3.54), 25.01 ± 6.79 (8.24–62.56) and 51.52 ± 13.82 (17.96–126.95), respectively. The average activity ratio $\pm$ standard error (range) of $^{234}U/^{238}U$, $^{226}Ra/^{238}U$, $^{210}Pb_{alpha}/^{238}U$ and $^{238}U/^{232}Th$ were 1.0 ± 0.05 (0.83–1.26), 0.96 ± 0.17 (0.48–1.55), 0.98 ± 0.18 (0.55–1.55) and $2.0\,8 \pm 0.90$ (0.43–5.61), respectively.

The concentration of uranium varies widely in natural waters due to its varied chemical behaviour in response to redox conditions. The oxidised U^{6+} (uranyl) ion complexes readily with carbonate, phosphate, or sulfate ion and is easily transported in the hydrologic cycle. In reducing waters, U^{4+} has an extremely strong tendency to precipitate and to remain immobile (Cowart and Burnett, 1994). The behaviour of uranium in aquatic systems is rather conservative and inert. The mean residence time for uranium in seawater is considered to be 5×10^3 years. Therefore, a relatively homogeneous distribution of uranium should be expected (Holm and Bojanowski, 1989).

Although the number of the analysed samples was limited, the uranium concentration varied widely from 9.72 to 61.98 Bq/kg dry weight. The main source of sediments to the beaches of the Egyptian Red Sea is the terrestrial deposits transported from the fringing mountains. The uranium concentration in the shore sediment depends on the uranium concentration in the fringing mountains (crystalline rocks), and the mobility of uranium from the rock and the shore sediment by rain and sea water, respectively (Strezov et al., 1996; El Mamony and Rifaat, 2001).

The average activity ratios of $^{234}U/^{238}U$, $^{226}Ra/^{238}U$ and $^{210}Pb_{alpha}/^{238}U$ are close to unity (1.00, 0.96 and 0.98, respectively), which imply that there is a secular equilibrium between ^{238}U and its progenies in the analyzed samples. The variation in these ratios could be due to the present of varying degrees of disequilibrium between the members of ^{238}U decay series in the coastal marine sediments (Higgy, 2000). Where leaching is less dominant, as in arid regions, the $^{234}U/^{238}U$ activity ratio become quite high. The key factors in the development of $^{234}U/^{238}U$ activity ratios out of equilibrium are the relative rate of leaching, mechanical erosion, and daughter half-life. Although the range of $^{234}U/^{238}U$ activity ratio varies greatly in surface water, often by factor of 2–3, the global average value is closely constrained at 1.2–1.3 (Ivanovich and Harmon, 1992). The activity ratios of

Table 4
Specific activity (Bq/kg dry weight) of U-238, U-235 and U-234, and activity ratios of U-234/U-238, U-235/U-238, Ra-226/U-238 and Pb-210/U-238 in shore sediment of the Egyptian Red Sea coast

Ser.	Code	U-238 ± E	U-235 ± E	U-234 ± E	Total U ± E	U-234/U-238	U-235/U-238	Ra-226/U-238	Pb-210/U-238
1	453	18.62 ± 1.86	<2.39	18.83 ± 1.87	37.45 ± 2.64	1.01	–	0.48	0.55
2	462	9.72 ± 1.5	<3.2	8.24 ± 1.36	17.96 ± 2.02	0.85	–	0.99	1.13
3	469	24.43 ± 1.98	2.87 ± 0.8	23.56 ± 1.60	50.86 ± 2.68	0.96	0.12	0.83	0.74
4	470	10.44 ± 1.61	<3.21	10.98 ± 1.65	21.42 ± 2.31	1.05	–	0.92	1.39
5	474	18.82 ± 1.74	3.54 ± 1.0	23.64 ± 2.21	46.00 ± 3.00	1.26	0.19	–	0.55
6	507	61.98 ± 3.9	2.41 ± 0.5	62.56 ± 3.94	126.95 ± 5.57	1.01	0.04	1.55	1.55
7	512	32.77 ± 3.29	<2.98	27.26 ± 2.88	60.03 ± 4.37	0.83	–	–	–

$^{238}U/^{232}Th$ varied widely over ten fold (0.43–5.61) with an average value of 2.08. The Th^{4+} is the only oxidation state of thorium and as such it is quite insoluble. Although transport of thorium in streams can occur by the movement of particulate matter to which the thorium is attached, in general the mobility of thorium is quite restricted (Cowart and Burnett, 1994). So, the geo-chemical behaviour of uranium and thorium could explain the wide variation in their activity ratios in shore sediment samples. The difference in their geo-chemical behaviour in marine environment is very obvious in the Red Sea bottom sediment where $^{238}U/^{232}Th$ average activity ratio is 40 (Khatir et al., 1998a,b).

Statistical analyses of the estimated parameters (activity of different radionuclides and their ratios) of the Red Sea coast shore sediment are given in Table 5. Average activities (range) of ^{226}Ra, ^{232}Th, ^{40}K, ^{238}U and ^{234}U (Bq/kg dry weight) in Red Sea shore sediment and soil, and Mediterranean Sea shore sediment (Alexandria City) and calculated absorbed dose rate (μGy/h) at 1 m above the ground due to natural radionuclides in sediment samples are given in Table 6.

Table 5
Statistical summary of estimated parameters of Red Sea Egyptian coast shore sediments

	Mean	SD[a]	SE[b]	Range	Unit	No.[c]
Ra-226	24.65	26.00	4.33	5.3–105.6	Bq/kg	36
Th-232	31.41	55.68	9.41	2.3–221.9	Bq/kg	35
K-40	427.48	213.10	35.52	97.6–1011	Bq/kg	36
Pb-210[d]	25.56	21.34	3.90	7.1–81.8	Bq/kg	30
Pb-210[e]	23.90	20.94	3.65	8.1–96.0	Bq/kg	33
U-238	25.25	18.04	6.82	9.7–62.0	Bq/kg	7
U-235	2.94	0.57	0.33	2.9–3.5	Bq/kg	3
U-234	25.01	17.96	6.79	8.2–62.6	Bq/kg	7
U-total	51.52	36.57	13.82	18.0–127.0	Bq/kg	7
Ra-226/Ra-228	1.67	1.19	0.20	0.4–5.3	–	35
Pb-210[d]/Ra-226	1.22	0.52	0.10	0.5–2.4	–	30
Pb-210[e]/Ra-226	1.48	0.74	0.14	0.5–4.4	–	30
Pb-210[e]/Pb-210[d]	1.28	0.43	0.09	0.6–2.5	–	2
U-234/U-238	1.00	0.14	0.05	0.8–1.3	–	7
U-235/U-238	0.11	0.07	0.04	0.04–0.19	–	3
Ra-226/U-238	0.96	0.39	0.17	0.5–1.6	–	5
Pb-210[e]/U-238	0.98	0.43	0.18	0.6–1.6	–	6
Absorbed dose rate	41.60	36.93	6.15	8.4–156.0	nGy/h	36
Radium equivalent activity	101.2	108.1	18.0	16.4–442.7	Bq/kg	36
Density	1.61	0.13	0.02	1.3–1.8	g/ml	40
CO_3	33.40	22.13	3.59	2.9–1269	%	38
Ba	2390.4	1357.8	223.2	183.6–5450	ppm	37
Sr	3676.9	2255.4	370.8	107.7–8073	ppm	37

[a] Standard deviation.
[b] Standard error.
[c] Number of analysed samples.
[d] Pb-210 gamma analysis.
[e] Pb-210 alpha analysis.

Table 6
Average specific activities (range) of ^{226}Ra, ^{232}Th, ^{40}K, ^{238}U and ^{234}U (Bq/kg dry weight) in Red Sea shore sediment and soil, and Mediterranean Sea shore sediment (Alexandria City) and calculated absorbed dose rate (μGy/h) at one meter above the ground due to natural radionuclides in sediment samples.

	Red Sea shore sediment	Red Sea Soil (Oil produced field)[a]	Mediterranean Sea (Alex.) shore sediment [b]
^{226}Ra	24.6 (5.2–105.6)	194,489	5.0 (3.0–10.8)
^{232}Th	31.4 (2.3–221.9)	897,803	2.1 (0.6–7.8)
^{40}K	427.5 (97.6–1011.3)	–	46.0 (10.0–86.1)
^{238}U	25.3 (9.72–62.0)	24.0	8.8 (3.6–13.8)
^{234}U	25.0 (8.2–62.6)	–	10.7 (3.7–17.5)
Absorbed dose rate	41.6 (8.4–156.0)	–	48.2 (19.3–117.5)

[a] Shawky et al. (2001).
[b] Higgy (2000).

4. Conclusions

Investigation of the radio-ecological characteristics of the Egyptian coast of the Red Sea and the radiological impacts of the non-nuclear industries (oil industries and phosphate mining) on the coastal environment are needed. The results of our study, which is a part of the national program for nuclear safety and radiation control, are a data-base to distinguish any future changes due to non-nuclear industries on the Red Sea coast. Our results imply that there is an indication of the radiological impacts of the oil industries in the Northern region of the Red Sea coast and phosphate mining in Safaga–Qusier region that need more detailed investigation on the pollution sources and the environmental distribution pattern of different pollutants. We are suggesting to study the impact of phosphate loading on the marine environment near Safaga port and the radio-chemical impacts of salt brines of water desalinization at Hurghada.

References

Cowart, J.B., Burnett, W.C., 1994. The distribution of uranium and thorium decay series radionuclildes in the environment—a review. Journal of Environmental Quality 23, 651–662.

Currie, L.A., 1968. Limits for detection and quantitative determination. Analytical chemistry 40 (3), 586–593.

El Mamoney, M.H., Rifaat, A.E., 2001. Discrimination of sources of barium in beach sediments, Marsa Alam to Shuqeir, Red Sea, Egypt. J. King Abdulaziz Univ. Marine Sciences 12, 149–160.

Hamilton, T.F., Smith, J.D., 1986. Improved alpha energy resolution for the determination of polonium isotopes by alpha-spectrometry. Applied Radiation and Isotopes 37 (7), 628–630.

Hanna, Reg, 1992. The level of heavy metals in the Red Sea after 50 years. Science of the total environment 125, 417–448.

Hawkins, J.P., Roberts, C.M., 1993. The growth of coastal tourism in the Red Sea: present and possible future effects on coral reefs. In: Ginsburg, R.N., W. Smith, F.G. (Eds.), In: Proceedings of the Colloquium on Global Aspects of Coral Reefs, Miami, 1993, (university of Miami, RSMAS), 1994, pp. 385–391.

Higgy, R.H., 2000. Natural radionuclides and plutonium isotopes in soil and shore sediments onAlexandria Mediterranean Sea coast of Egypt. Radiochim Acta 88, 47–54.

Holm, E., Bojanowski, R., 1989. Natural activity in the Baltic Sea. In: The Radioecology of Natural and Artificial Radionuclides, Proceeding of the XV Regional Congress of IRPA, Vishy, Sweden, pp. 49–54.

Hussain, N., Kim, G., Church, T.M., Carey, W., 1996. A simplified technique for gamma-spectrometric analysis of ^{210}Pb in sediment samples. Applied Radiation and Isotopes 47 (4), 473–477.

Ibraheim, N.M., Abd El Ghani, A.H., Shawky, S.M., Ashraf, E.M., Farouk, M.A., 1993. Measurement of radioactivity levels in soil in the Nile Delta and Middle Egypt. Journal Health Physics 64 (6), 620–627.

Intergovernmental Oceanographic Commission (of UNESCO), 1997. Regional blueprint and pilot projects for the Red Sea, Fourth Session of the GOOS Health of the Oceans Panel, the National University of Singapore, 13–17 October 1997. (http://ioc.unesco.org/ goos/hoto4_toc.htm).

Ivanovich, M., Harmon, R.S., 1992. Uranium Series Disequilibrium: applications to Earth, Marine and Environmental Sciences, second ed . Clarendon press, Oxford.

Khater, A.E.M., 1997. Radiological study on the environmental behaviour of some radionuclides in the aquatic ecosystem. Ph.D. thesis, Cairo University.

Khater, A.E.M., Ashraf, R.H.H., Pimpl, M., 2001. Radiological impacts of natural radioactivity in Abu Tartor posphate deposits, Egypt. Journal Environmental Radioactivity 55, 255–267.

Khatir, S.A., Ahamed Mustafa, M.O., El-Khaangi, F.A., Nigumi, Y.O., Holm, E., 1998a. Radioactivity levels in the Red Sea coastal environment of Sudan. Marine Pollution Bulletin 36 (1), 19–26.

Khatir, S.A., El-Ganawi, A.A., Ahamed, M.O., El-Khaangi, F.A., 1998b. Distribution of some natural and anthropogenic radionuclides in Sudanese harbour sediments. Journal of Radioanalytical and Nuclear chemistry 237 (1–2), 103–107.

National Academy of Science (1999). Evaluation of guidelines for exposure to technologically enhanced naturally occurring radioactive materials. http://www.nap.edu/ openbook/0309062977.

Pimpl, M., Yoo, B., Yordanoua, I., 1992. Optimisation of radioanalytical procedure for the determination of uranium isotopes in environmental samples. Journal of Radioanalytical chemistry 161 (2), 493–501.

Said, R., 1990. The geology of Egypt, A.A. Balkema/Rotterdam/Brookfield.

Shawky, S., Amer, H., Nada, A.A., Abd El-Maksoud, T.M., Ibrahium, N.M., 2001. Characteristics of NORM in the oil industry from Eastern and Western deserts of Egypt. Applied Radiation and Isotopes 55, 135–139.

Strezov, A., Yordanov, M., Pimpl, M., Stoilova, T., 1996. Natural radionuclides and plutonium content in Black Sea bottom sediments. Journal of Health Physics 70 (1), 70–80.

United Nations Scientific Committee on the Effects of Atomic Radiation, (2000). Sources and effects of ionising radiation. Report to the general assembly with annexes, UNSCEAR 2000.

United States Department of Energy, 1992. EML procedures manual. Report HASL 300.

Vegueria, Jerez, S.F., Godoy, J.M., Miekeley, N., 2002. Environmental impact study of barium and radium discharges by produced waters from the "Bacia de Campos" oil-field offshore platforms, Brazil. Environmental Radioactivity 62, 29–38.